

# Benoit Beckers

Architecture et Physique Urbaine - ISA BTP  
Université de Pau et des Pays de l'Adour  
Allée du Parc Montaury, 64600 Anglet (France)  
[benoit.beckers@univ-pau.fr](mailto:benoit.beckers@univ-pau.fr), [www.heliodon.net](http://www.heliodon.net)

## Finite Element Simulation of Transient Heat Transfers

*Dual Analysis for Heat Conduction Problems by Finite Elements*, **B. Fraeijs de Veubeke & M. Hogge**, IJNME, 1972

*A 33 line heat transfer finite element code*, **P. Beckers & B. Beckers**, Report Helio 010, 2016

*A 66 line heat transfer finite element code to highlight the dual approach*, **P. Beckers, B. Beckers**, Computers & Mathematics with Applications, Volume 70 Issue 10, November 2015, Pages 2401-2413.

## Worldwide aspects of solar radiation impact

Any thermal state can be modeled as a system subjected to cyclic flows of mass and energy. **The earth is** a sphere almost smooth, slightly flattened at the poles, which rotates around the sun in a slightly elliptical path. This is **the largest thermal system that we have to deal with**, the one that determines all the others: territory, city, building, machinery, plant or animal.

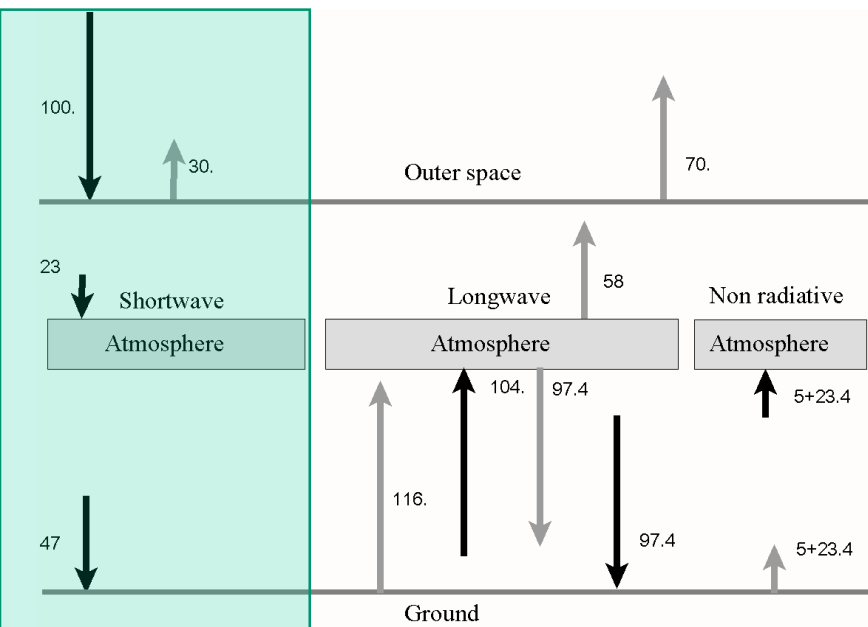
### Global energy budget at the Earth level

The distance between the earth and the sun is about 150 millions of kilometers (1 AU: Astronomical Unit) and the radius of the earth is approximately 6370 km. The earth rotates on itself in just less than 24 hours (1 day), and around the sun in the ecliptic plane, with a period of about 365.25 days. The axis of the first rotation (which defines the two poles) is tilted 23.5 degrees relative to the normal to the ecliptic plane. This obliquity determines the peculiar tropical latitudes (23.5 ° with respect to the equator) and the polar circles (23.5 ° with respect to the poles, and thus 66.5 ° from the equator).

The surface of the sun behaves approximately like a blackbody with a temperature of 5780 K. By the Stefan-Boltzmann law, we deduce that a unit area located at the distance of 1 AU, set perpendicular to the sunray, intercepts a power of **1367 W/m<sup>2</sup>**. The emitted spectrum has its maximum to 500 nm (wavelength of yellow perceived by the human eye) and is divided almost equally in visible light and near infrared ( $\lambda < \mu 4$ ), with a small amount of ultraviolet.

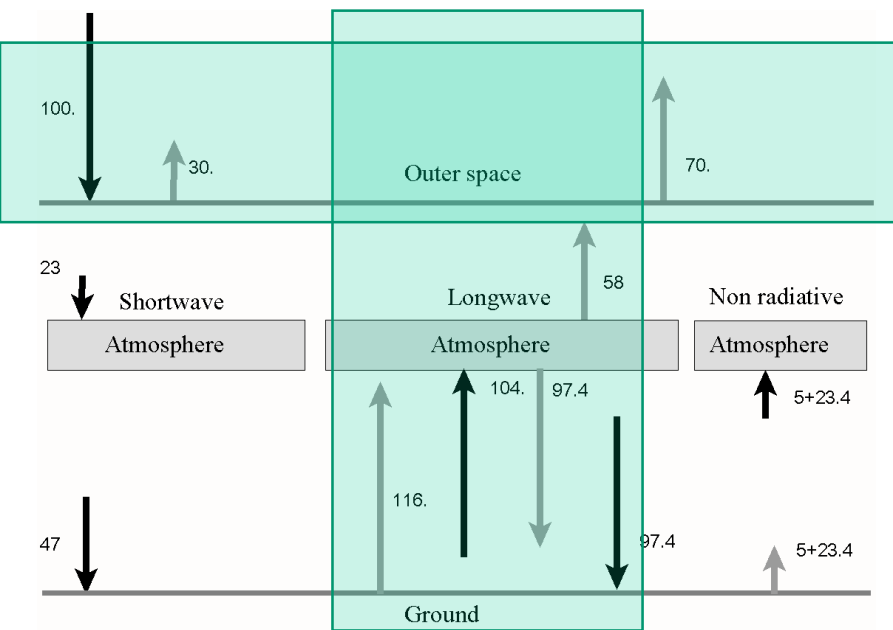
The solar constant ( $1367 \text{ W/m}^2$ ) is equivalent to the average irradiance that can be captured in the vicinity of the earth. It varies from about 6.9% during the year due to the elliptic shape of the earth's orbit ( $1412 \text{ W/m}^2$  in early January to  $1321 \text{ W/m}^2$  in July) and very little in the long term. Atmospheric absorption and inclination of the receiving surface relative to the direction of radiation generate significant weakening.

To deduce the average solar illumination of the planet, at the top of the atmosphere, it is sufficient to consider that the sun sees the earth as a disk, irradiated at a rate of  $1367 \text{ W/m}^2$ , but that radiation actually reaches a sphere of same radius, and thus a four times larger area. The average sunshine is therefore  $342 \text{ W/m}^2$ . It is understood that it is not uniform – the equator receives more than the poles – but this value is used to describe an average annual radiation balance for the entire earth-atmosphere system.



The top of the atmosphere receives, therefore,  $342 \text{ W/m}^2$ . For clarity of reasoning, all flows are expressed as percentages of this value. Over the year, the same amount of energy that comes from the sun must be lost to space by the earth-atmosphere system (EA). The clouds reflect back into space about 23% of the incoming flow and absorb about 23%, the remaining half reaches the earth's surface, which reflects about 7% of the flow and absorbs the remaining 47%.

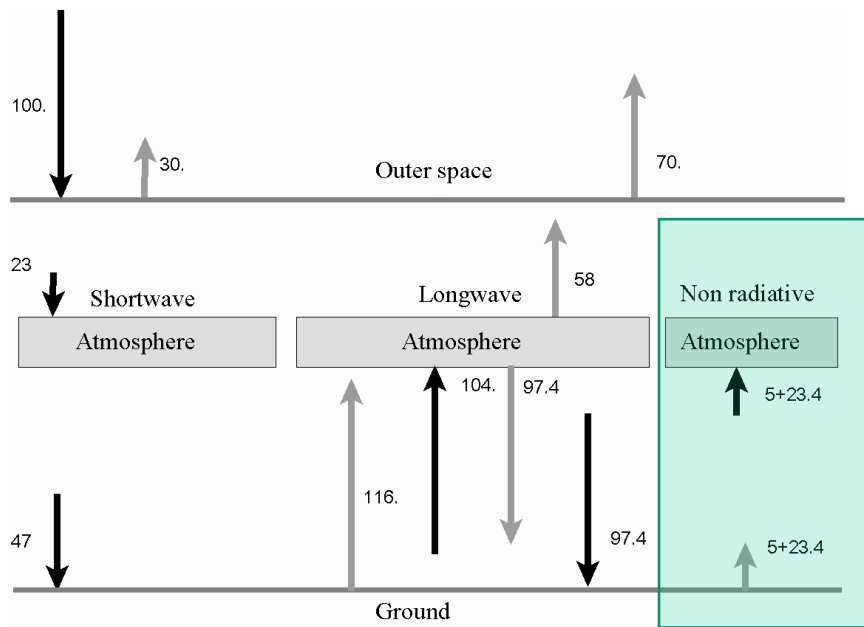
In total, 30% of the flux is reflected and therefore does not take part in the energy balance of the EA system. The atmosphere, which absorbs only a quarter of the flow, can be considered as semi-transparent to shortwave solar radiation, and is therefore not heated by it. In contrast, almost half of the flux is absorbed at the surface of the earth.



The earth has an average temperature of about 288 K. It therefore emits in long waves ( $\lambda > 4\mu$ ); for this region of the spectrum, it behaves almost like a blackbody: snow, water, vegetation or rock have an emissivity almost unitary in the far infrared.

Earth's surface emits more in the range of long wave (116%) than it receives in the shortwave range above the atmosphere, because it also receives long wave of the atmosphere, in fact, only a small part of its emission escapes into space, while most is absorbed by the atmosphere (104%). The atmosphere radiates into space in longer wavelengths (70%) and to the surface of the Earth (97.4%), with a total of 167.4%.

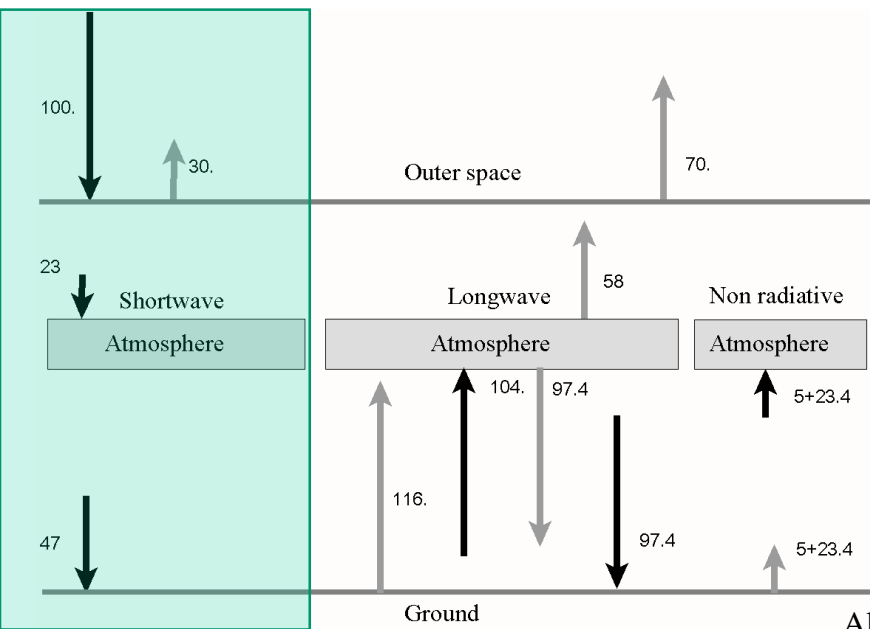
In total, the EA system is in radiative equilibrium, since the solar irradiation (100%) is equal to the sum of shortwave reflection (30%) and long-wave emission of the earth and atmosphere (70%).



In contrast, the sub-systems consisting of the earth and the atmosphere are not in equilibrium. The earth's surface receives 47% of the shortwave radiation, but its emission in long wave is only 18.6% (116% to the atmosphere, from which it receives 97.4% back). **All wavelengths combined, the earth has a positive balance of 28.4%.**

The atmosphere, however, wins 23% by absorption of clouds and constituents, but loses 51.4% in the long waves (it absorbs 104% of the terrestrial surface, but emits  $97.4 + 58 = 155.4\%$  to space and surface of the earth). **The balance of atmospheric subsystem is negative: - 28.4%.**

**Convection** carries the excess energy from the earth's surface to the atmosphere, in the following proportions: **5% as sensible heat** and **23.4% as latent heat**. Note finally that the **heat conduction** in the soil does not get involved, because the net storage of heat in the earth's surface does not vary over the annual period.



All these data are shown in more details in Table 1 from reference [TRE 09]. They are reproduced in  $\text{W/m}^2$  and percentages. Their examination shows that the record is not entirely accurate: there is a slight excess of radiation absorbed by the earth equal to  $0.9 \text{ W/m}^2$ .

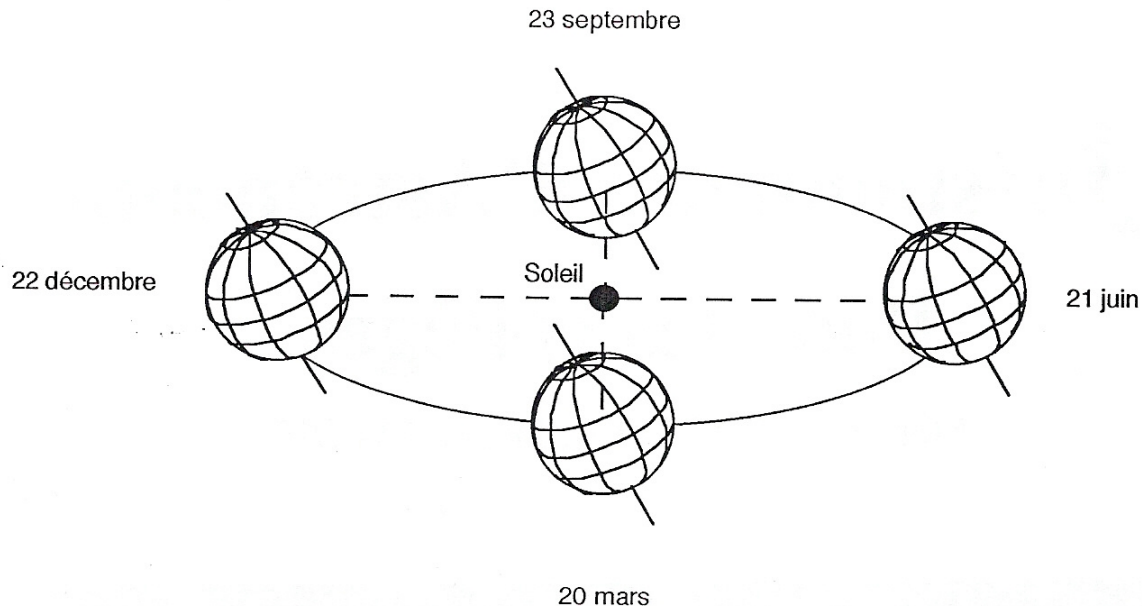
Table 1. Average rate of radiative exchanges

Trenberth <i>et al.</i>	$\text{W/m}^2$	%
Incoming solar radiation	341.3	100
Reflected solar radiation (a + b)	101.9	30.
a) Reflected by clouds and atmosphere	79	23.1
b) Reflected by surface	23	6.75
Absorbed by surface	161	47.2
Absorbed by atmosphere	78	22.9
Thermals (sensible)	17	5
Latent heat	80	23.4
Surface radiation	396	116
Surface radiation to atmosphere	356	104
Surface radiation to sky	40	11.7
Outgoing longwave radiation	238.5	70
Emitted by atmosphere (and clouds)	169+30	58.3
Back radiation	333	97.6

## The distribution of solar radiation on Earth's surface

Solar radiation reaches the earth with a variable incidence (angle between the solar ray and the normal to the earth's surface). This incidence increases as one moves away from the earth - sun axis by going to the edge of the sphere. Because the axis of rotation of the earth is tilted on its orbit around the sun, the earth - sun axis moves during the year, its position varies between the two tropics.

The sun crosses the zenith a few days per year for all points between the tropics. The further away from the equator, the sun drops over the horizon, and increases the contrast between summer and winter. At the poles, there is only one day and one night that share the year.





By calculating the irradiance on a horizontal plane at the top of the atmosphere as a function of latitude, we obtain the results summarized in *Fig. 1*. [PET 06]. They correspond to the solar constant of  $1367 \text{ W/m}^2$ . The calculation is based on the actual elliptical orbit of the earth (see Chapter 10). Note that the average daily irradiance is much greater during the southern summer than during the northern summer. This is because the earth passes closer to the sun earlier in the year than at the beginning of July. The irradiance varies inversely as the square of the distance, that is to say, in the ratio of 1.07 (*Fig. 1*).

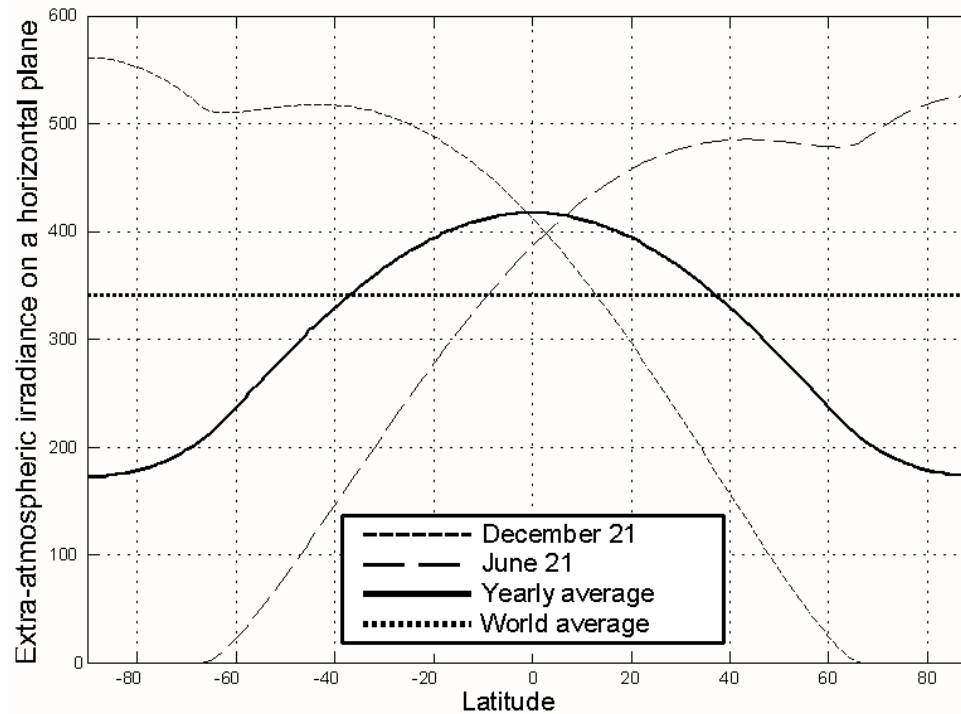


*Fig. 1. Average daily solar irradiance ( $\text{W/m}^2$ ) above the atmosphere as a function of latitude during the solstices and on average over the year*

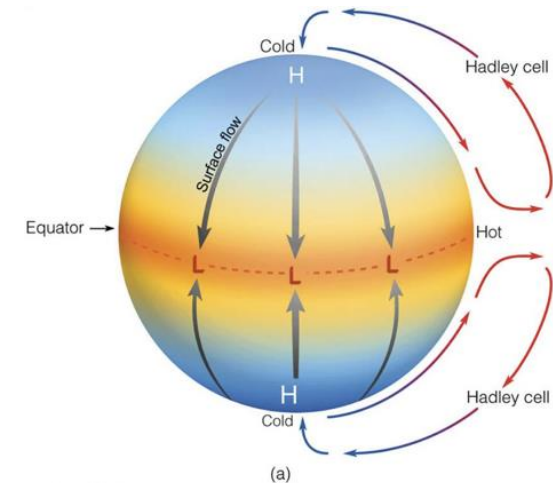
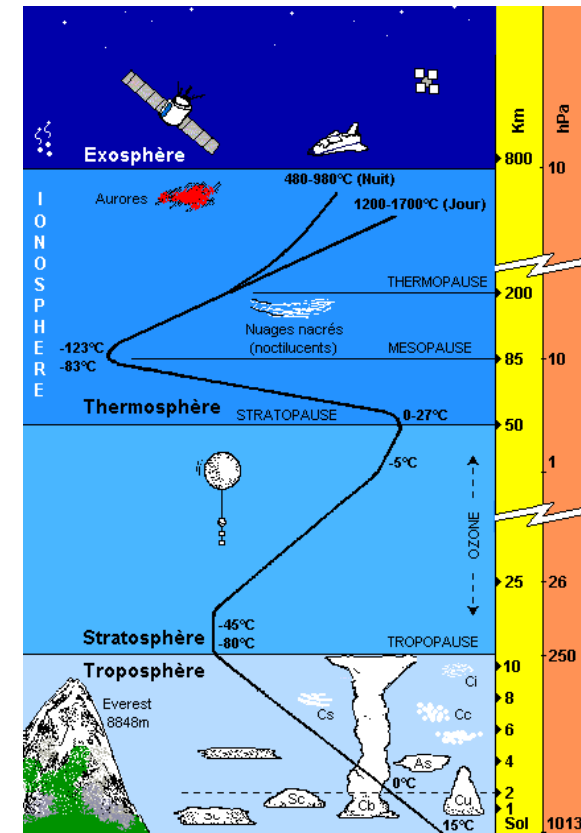
It should be noted that the result in *Fig. 1* is not valid at ground level, because, even during a sunny day, the atmosphere produces an attenuation of solar radiation which depends on the orientation of the solar ray and therefore on the length of its path through the atmosphere [CAM 98].

## 2.1. Consequence of the unequal distribution of sunshine

The earth is surrounded by an atmosphere whose composition varies with altitude. There are several layers. The lowest is called the troposphere. Its thickness is on average equal to 12 km, but it reaches 15-20 km between the tropics and only 7-10 km at the poles [WAU 00, MON 07].

The non uniform distribution of solar radiation causes atmospheric advection currents that tend to balance important air masses [WAL 06]. Hotter zones near the equator give rise to significant thermals that reach the limits of the troposphere where the air is pushed northward or southward. Indeed, in the region between the tropics, annual average irradiance at the top of the atmosphere is nearly 30% higher than at latitude of 40 ° and 50% higher than at latitude 50 °.

The air mass gradually cools as it moves poleward. In the absence of other phenomena, one could imagine an upper flow from the equator to the poles and a return toward the equator in the lower layers of the atmosphere (Hadley cell). This situation is observed on the planet Venus, where there is a single Hadley cell in each hemisphere.



## 2.2. Effect of Earth rotation

Because of the influence of earth rotation, which deflects the atmospheric motions clockwise in the northern hemisphere and anticlockwise in the southern hemisphere, the movement is more complex and takes place on the basis of the tri-cellular atmospheric model [WAU 00].

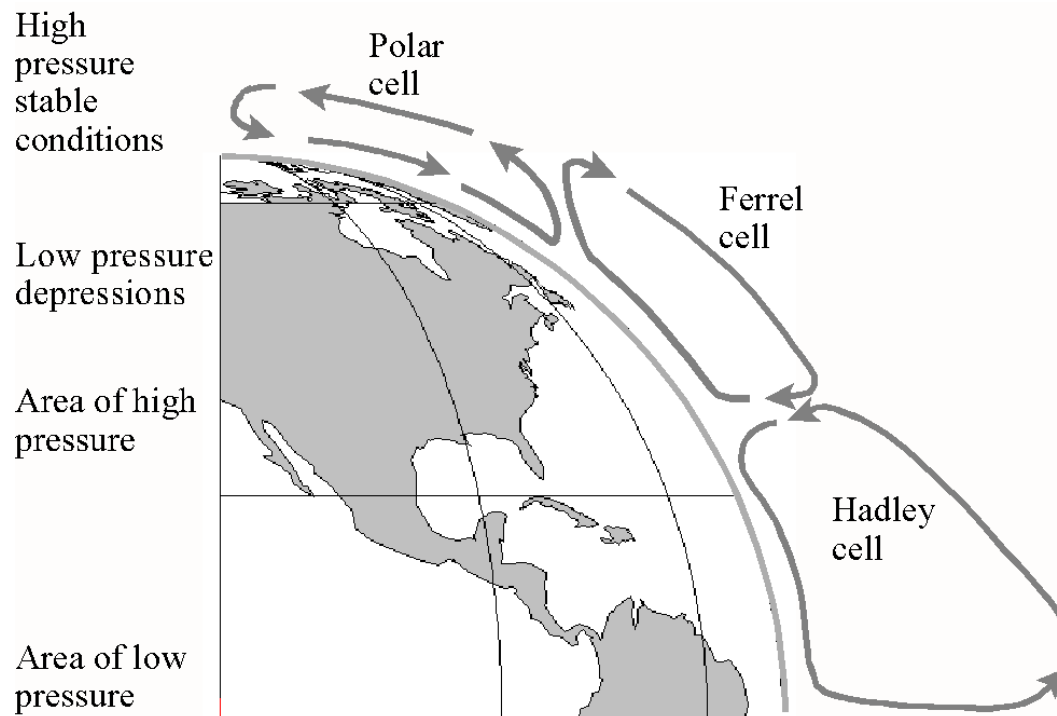
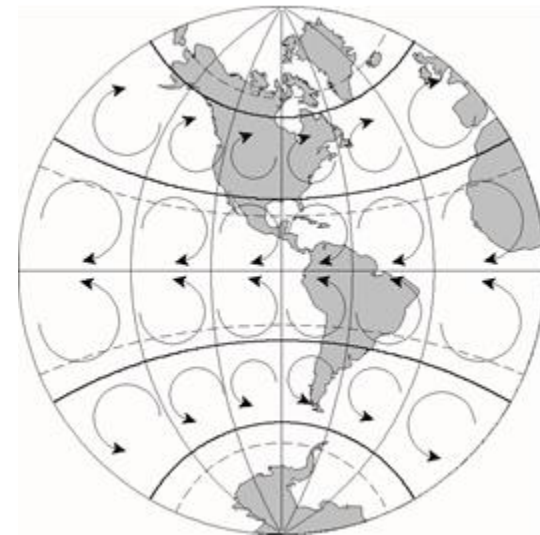
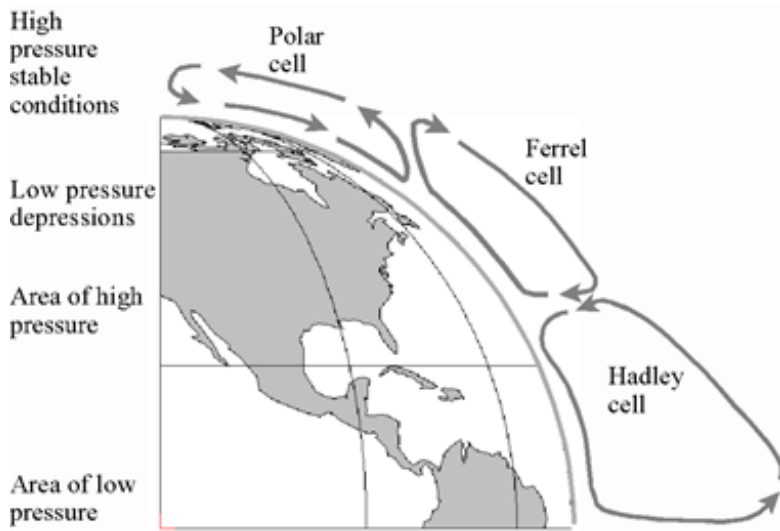
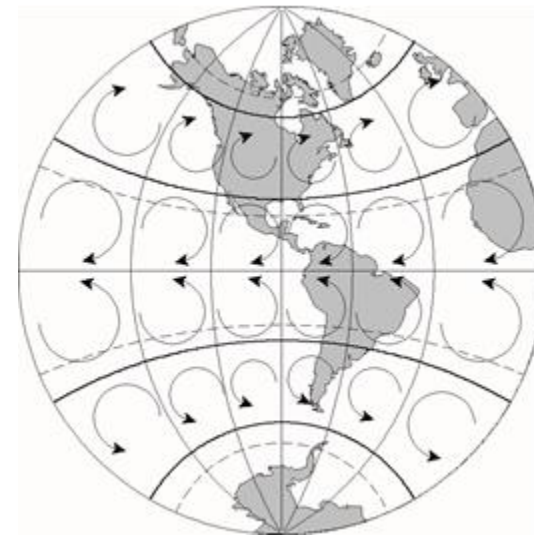
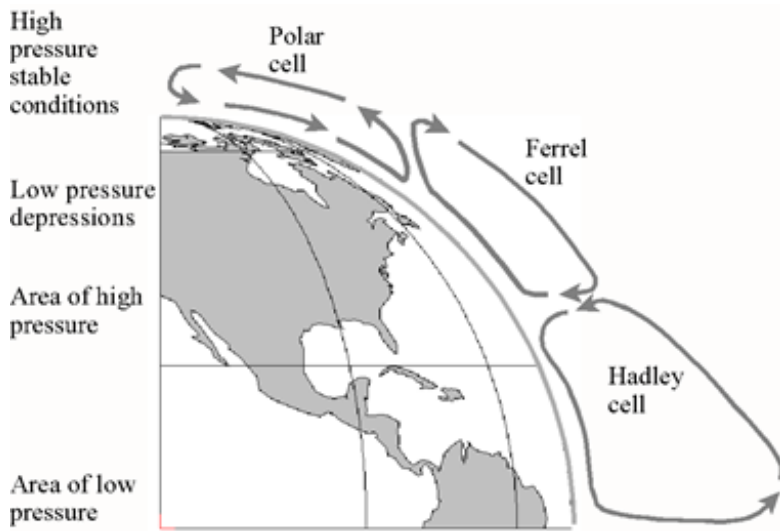


*Fig.1. Tri-cellular model of atmospheric circulation*

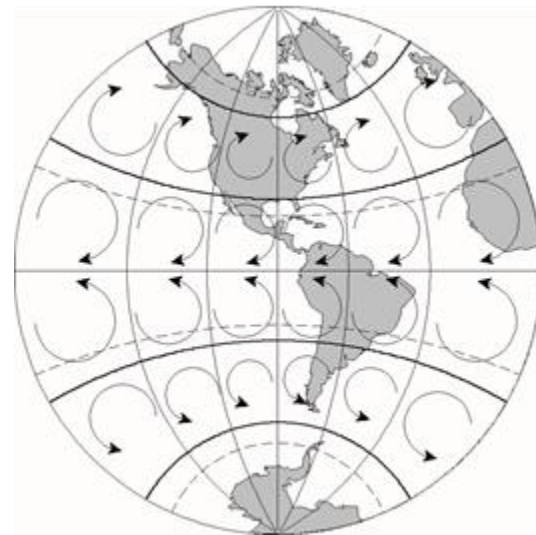
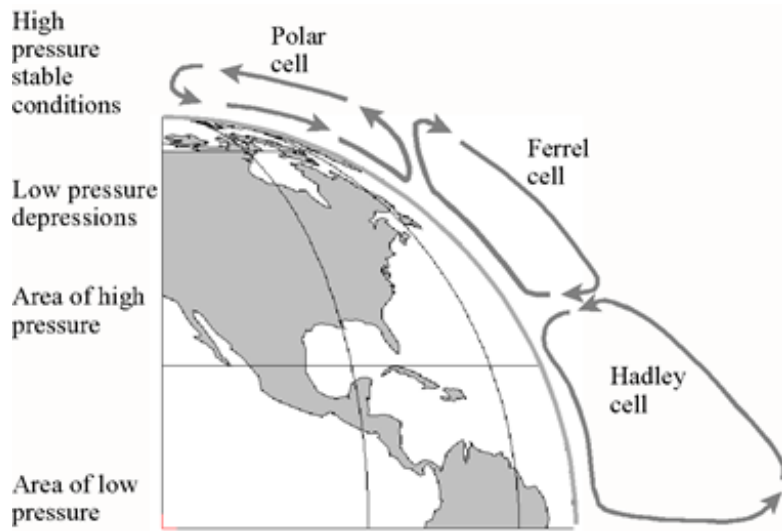


The deviation caused by the Coriolis force is easily explained. First note that the tangential velocity of a point on the earth is oriented from west to east. On the equator, it is equal to  $40000 \text{ km} / 24 \text{ h} = 1666 \text{ km/h}$  or  $463 \text{ m/s}$  (faster than the speed of sound:  $340 \text{ m/s}$  at sea level). This speed varies with latitude  $\alpha$ , it is equal to  $v_{equator} \cos \alpha$  (at  $60^\circ$  latitude, it is thus equal to half its value on the equator).

In the northern hemisphere, the tangential velocity of a point on the earth therefore decreases as one travels northward. However, the airstream will keep the same speed, implying that the earth is behind the movement and that air moves eastward (right) in the terrestrial frame. While traveling north-south, the air stream is delayed, since the linear velocity of the soil increases, so the stream deflects westward (right). In the southern hemisphere, the phenomenon is reversed.



The terrestrial sphere is subjected to regimes of low pressure at the equator and parallels 60 ° north and south. High pressures are present at parallels 30 ° and in the northern and southern poles as well. Warm air rises in the equatorial low pressure zone, and then it cools as it moves at higher altitudes to the north. It goes down into areas of high pressure located just north of the tropic and returns toward the equator as trade winds. Except in the equatorial zone, where its effect is not perceptible, the Coriolis force deflects winds clockwise in the Northern Hemisphere and anticlockwise in the Southern Hemisphere. In the northern hemisphere, the winds come from the north-east and head to the southwest.



The atmospheric movement we could observe in a meridian plane is shown schematically in *Fig.left*. It shows the three conventional cells: Hadley, Ferrel and polar cell. In the equatorial zone, the movement is fairly stable, but it is not the same in areas closer to the poles, where oscillations are occurring.

Movements therefore tend to follow trajectories similar to those shown in *Fig.right*. In this figure, the parallels drawn in dotted lines represent the tropics; those who are in solid lines correspond to latitudes of  $\pm 30^\circ$  and  $\pm 60^\circ$ .

The local climates depend in first approximation on the latitude. The equator is hot and humid (with the large forests of Amazonia, Congo and Indonesia), meanwhile the tropics, subject to the rules of the trade winds, are divided between humid climates, as these found near the sea, and the driest climates in the world. The largest deserts of the world (Sonora, Sahara, Gobi in the northern hemisphere; Atacama, Kalahari, Australia in the southern one) are found around the tropics. To 30 or 40 degrees latitude, there are still deserts, but also the warm temperate climate of the Mediterranean.

This pattern of air currents can be explained by the distribution of solar irradiance at ground level as a function of latitude. Indeed, we see that the maximum irradiance occurs in the tropics. This is because cloud cover is always important at the equator (low pressure area) and generally low in the tropics (high pressure areas).

### ***2.3. Influence of continental masses***

The climate is also influenced by the proximity of the oceans and the presence of major marine currents. The distribution of land and ocean is very different in both hemispheres [GOD 09]. This is clearly seen in *Fig.1*. To make the figure readable, we use the equal-area azimuthal projection, also known as Lambert projection, which respects the proportions of areas. This uneven distribution combined with the action of air currents is the cause of ocean currents.

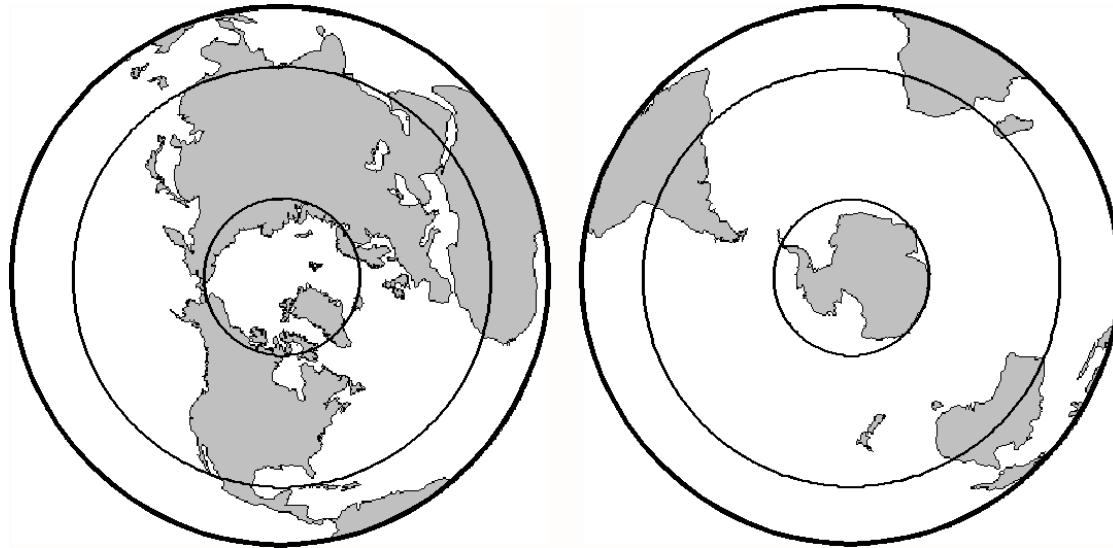
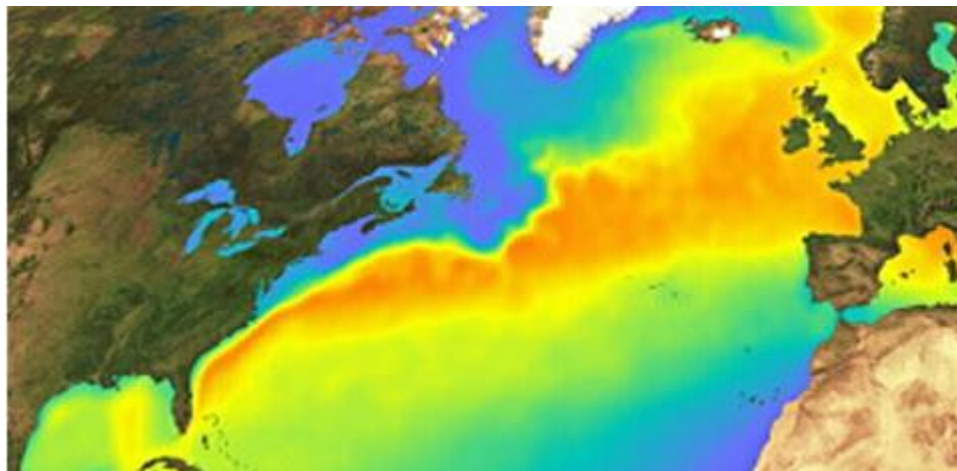


*Fig.1. Comparison of lands and seas areas in both hemispheres*



The cold-temperate zone starts around 50 degrees. In the southern hemisphere, there is no more land, while the northern hemisphere extends to a polar region where there are still significant populations. At the same latitude, Europe is favored by the Gulf Stream circulation, especially compared to the east coast of North America, which suffers the opposite effects (New York, where it snows regularly in winter, is 40 ° North latitude as well as Rome, Barcelona and Beijing). The Humboldt

Current cools strongly the Pacific off Chile and Peru. There are occurring cyclical and complex phenomena, like El Niño and La Niña, which are just beginning to be incorporated into global climate models. They show how local thermal imbalances can have consequences far away, for example on the monsoon regime in India or on the drought in east Africa.



To carry out the transient studies, new physical quantities, such as the **density of the material** and its **heat capacity**, are introduced.

Let us consider an isotropic body with heat conduction coefficient  $k$  ( $Wm^{-1}K^{-1}$ ) and volume heat capacity  $c_v$  ( $JK^{-1}m^{-3}$ ). The transient heat conduction equations are:

$$k \Delta \tau + Q = c_v \frac{\partial \tau}{\partial t}$$

The variable  $Q$  ( $Wm^{-3}$ ) represents the heat source that has not yet been used in these lectures.

In the lack of heat source, the equation becomes:

$$\frac{\partial \tau}{\partial t} = \frac{k}{c_v} \Delta \tau$$

This equation depends on a single material characteristic : the ratio  $k/c_v$ , which is called **thermal diffusivity**.

The **thermal diffusivity**  $\alpha$  of a material, expressed in  $m^2s^{-1}$ , represents its tendency to facilitate the diffusion of heat (a "good" thermal diffusivity in construction corresponds to a low value and a "bad" thermal diffusivity corresponds to a high one).

$$\alpha = \frac{k}{\rho c_p} = \frac{k}{c_v}$$

To switch from the local form of the differential equations

$$k \Delta \tau + Q = c_v \frac{\partial \tau}{\partial t} \quad (1)$$

and its **initial** and **boundary** conditions to the discretized formulation, two methods are available.

The first one follows the same path as the variational methods seen before for the stationary heat transfer. This formulation was presented by M [Biot in 1957](#) in a famous paper in the Journal of Aeronautical Sciences : *New Methods in Heat Flow Analysis With Application to Flight Structures*.

The second one which is more classical in the presentations of dynamic problems, is based on the **Galerkin** method. This is the formulation presented in the book of [Lewis et al: Fundamentals of the Finite Element Method for Heat and Fluid Flow \(2004\)](#). *See § 6,3,2 pp 153*.

# Galerkin method

The temperature is discretized as follows:

$$\tau(x, y, z, t) = \sum_{i=1}^n f_i(x, y, z)T_i(t) = [F][T]$$

where  $f_i$  are the shape functions,  $n$  the number of nodes in an element and  $T_i(t)$  the time dependent nodal temperatures. The Galerkin representation of equation (1) is:

$$\int_{\Omega} f_i \left[ k \Delta \tau + Q - c_v \frac{\partial \tau}{\partial t} \right] d\Omega = 0$$

We note above the concept of weighed residual with the shape functions used as weight functions. Employing integration by parts (*Lewis et al*) on the first term of the previous equation, we get:

$$[C] \left[ \frac{\partial [T]}{\partial t} \right] + [K][T] = [g] \quad (2)$$

In lecture 1, we have seen that:

$$[K] = \int_V k \text{grad} [F]^T \text{grad} [F] dV$$

where  $[F]$  is defining the blending functions of the temperature field.

We also see that the time dependent term of the differential equation will be taken into account through the use of a capacity matrix defined as follows

$$[C] = \int_V c_v [F]^T [F] dV$$

The second member  $[g]$  of equation (2) represents all the heat loads coming from the internal sources and the boundary conditions

# Time discretization using the Finite Difference Method

Between the  $n$  and  $n+1$  time levels, using a Taylor series, we can write:

$$\left[ T^{n+1} \right] = \left[ T^n \right] + \delta t \frac{\partial \left[ T^n \right]}{\partial t} + \frac{\delta t^2}{2} \frac{\partial^2 \left[ T^n \right]}{\partial t^2} + \dots$$

If the second and higher-order terms are neglected:

$$\frac{\partial \left[ T^n \right]}{\partial t} = \frac{\left[ T^{n+1} \right] - \left[ T^n \right]}{\delta t} + O(\delta t^2)$$

We finally obtain:

$$\left[ C \right] \left[ \frac{\partial \left[ T \right]}{\partial t} \right] + \left[ K \right] \left[ T \right] = \left[ g \right] \rightarrow \left[ C \right] \left\{ \frac{\left[ T^{n+1} \right] - \left[ T^n \right]}{\delta t} \right\} + \left[ K \right] \left[ T^\theta \right] = \left[ g^\theta \right]$$

We have just introduced a parameter  $\theta$  to get the value of  $[T]$  inside the interval:

$$\left[ T^\theta \right] = \theta \left[ T^{n+1} \right] + (1 - \theta) \left[ T^n \right]$$

$$[C] \left\{ \frac{[T^{n+1}] - [T^n]}{\delta t} \right\} + [K][T^\theta] = [g^\theta]$$

The development completed by Lewis *et al.* leads to the discretized equation (Lewis, equation 6.37):

$$([C] + \theta \delta t [K]) [T^{n+1}] - ([C] - (1 - \theta) \delta t [K]) [T^n] = \delta t (\theta [g^{n+1}] + (1 - \theta) [g^n])$$

The value of the tuning parameter  $\theta = 1$ , corresponds to the implicit scheme considered as unconditionally stable. We write:

$$([C] + \delta t [K]) [T^{n+1}] = [C] [T^n] + \delta t [g^{n+1}]$$

Dimensional analysis.

In the first line : the equation and

in the second one : the dimensions of the terms that compose it.

$$[C][T^{n+1}] + \delta t [K][T^{n+1}] = [C][T^n] + \delta t [g^{n+1}]$$

$$[JK^{-1}][K] = [J] \quad s[WK^{-1}][K] = [J] \quad [JK^{-1}][K] = [J] \quad s[W] = [J]$$

If we have fixed temperatures (not necessary) the vector  $[T]$  can be divided into two parts:

1. the unknown temperatures  $T_1$  and
2. the fixed and therefore constant temperatures  $T_f$ . So we rewrite:

$$\left( [C_{11} \quad C_{1f}] + \delta t [K_{11} \quad K_{1f}] \right) \begin{bmatrix} T_1^{n+1} \\ T_f \end{bmatrix} = [C_{11} \quad C_{1f}] \begin{bmatrix} T_1^n \\ T_f \end{bmatrix} + \delta t [g^{n+1}]$$

The superscripts  $n$  or  $n+1$  indicate the iteration. Developing for the lines corresponding to the unknowns:

$$[C_{11}] [T_1^{n+1}] + \delta t [K_{11} \quad K_{1f}] \begin{bmatrix} T_1^{n+1} \\ T_f \end{bmatrix} = [C_{11}] [T_1^n] + \delta t [g^{n+1}]$$

$$\left( [C_{11}] + \delta t [K_{11}] \right) [T_1^{n+1}] = [C_{11}] [T_1^n] - \delta t [K_{1f}] [T_f] + \delta t [g^{n+1}]$$

If there are **no loads nor fixations, only initial conditions**, we can remove the indices and we obtain the very simple equation:

$$\left( [C] + \delta t [K] \right) [T^{n+1}] = [C] [T^n]$$



Coming back to the capacity matrix  $[C]$ , we know that it is a function of the density  $\rho$  of the material, its heat capacity  $c_p$  and its volume  $V$ .

$$[C] = \int_V \rho c_p [F]^T [F] dV$$

$$\tau = T_1 \left(1 - \frac{x}{a}\right) \left(1 - \frac{y}{b}\right) + T_2 \frac{x}{a} \left(1 - \frac{y}{b}\right) + T_3 \frac{x}{a} \frac{y}{b} + T_4 \left(1 - \frac{x}{a}\right) \frac{y}{b}$$

$$\tau = [F][T]$$

$$[F] = \left[ \begin{array}{cccc} \left(1 - \frac{x}{a}\right) \left(1 - \frac{y}{b}\right) & \frac{x}{a} \left(1 - \frac{y}{b}\right) & \frac{x}{a} \frac{y}{b} & \left(1 - \frac{x}{a}\right) \frac{y}{b} \end{array} \right]$$

$$[T]^T = [T_1 \quad T_2 \quad T_3 \quad T_4]$$

To show the process of integration, we compute the term  $C_{33}$  of the capacity matrix  $[C]$ . The volume  $V$  is the product of the area  $ab$  by the thickness  $e$ .

$$C_{33} = e \int_0^a \left( \int_0^b \rho c_p \frac{x^2 y^2}{a^2 b^2} dy \right) dx$$

$$= \rho e c_p \int_0^a \frac{b^3 x^2}{3a^2 b^2} dx = \rho e c_p \frac{b}{3} \int_0^a \frac{x^2}{a^2} dx = \rho e c_p \frac{ab}{9} = \frac{\rho V c_p}{9}$$

It can be verified in this expression that the sum of its terms is equal to 36, and therefore, that concentrated in 1 point, the capacity would be equal to  $\rho V c_p$ . The matrix  $[C]$  is expressed in  $JK^{-1}$ .

$$[C] = \frac{\rho V c_p}{36} \begin{bmatrix} 4 & 2 & 1 & 2 \\ 2 & 4 & 2 & 1 \\ 1 & 2 & 4 & 2 \\ 2 & 1 & 2 & 4 \end{bmatrix}$$

Examples:

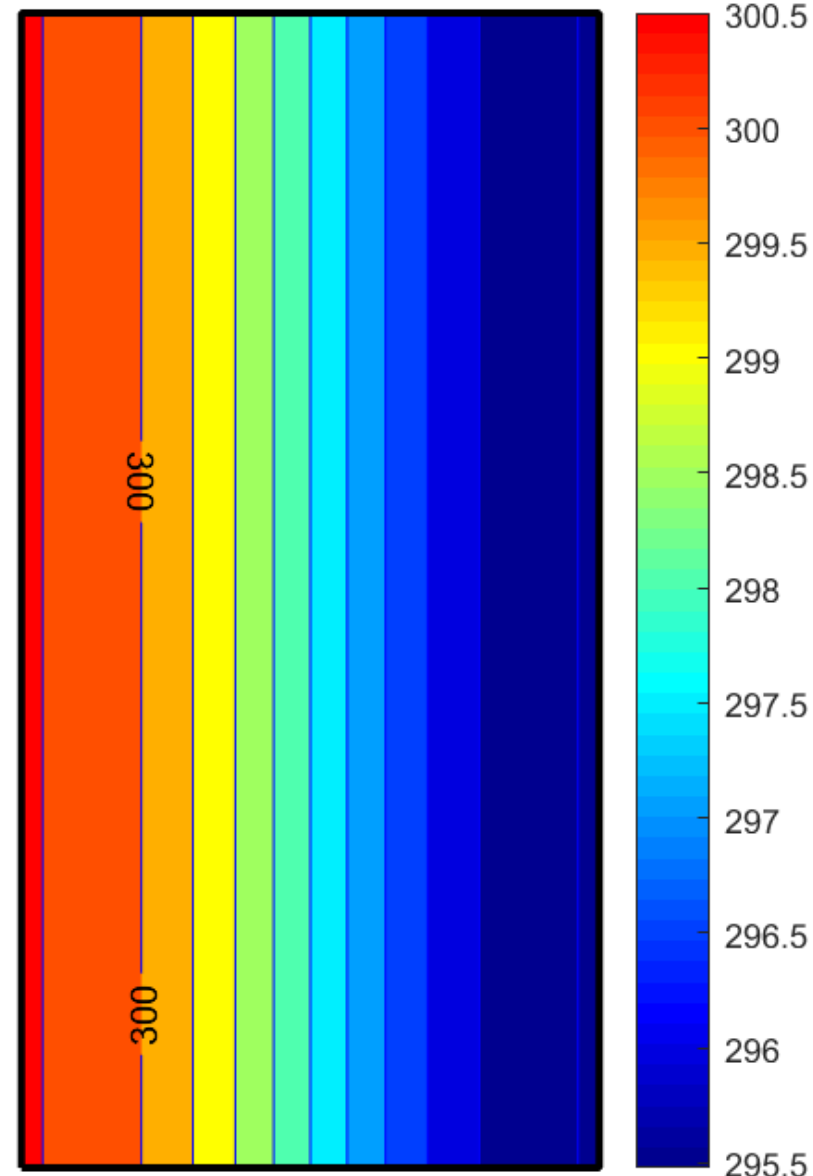
1. Homogenization of the temperature in an adiabatic domain
2. Heating of a cold domain
3. Cooling of a hot domain
4. Convection on three sides of the domain

$T_{\max} : 301 \text{ K}, T_{\min} : 295 \text{ K}, \text{ pas} : 0.5 \text{ K}$

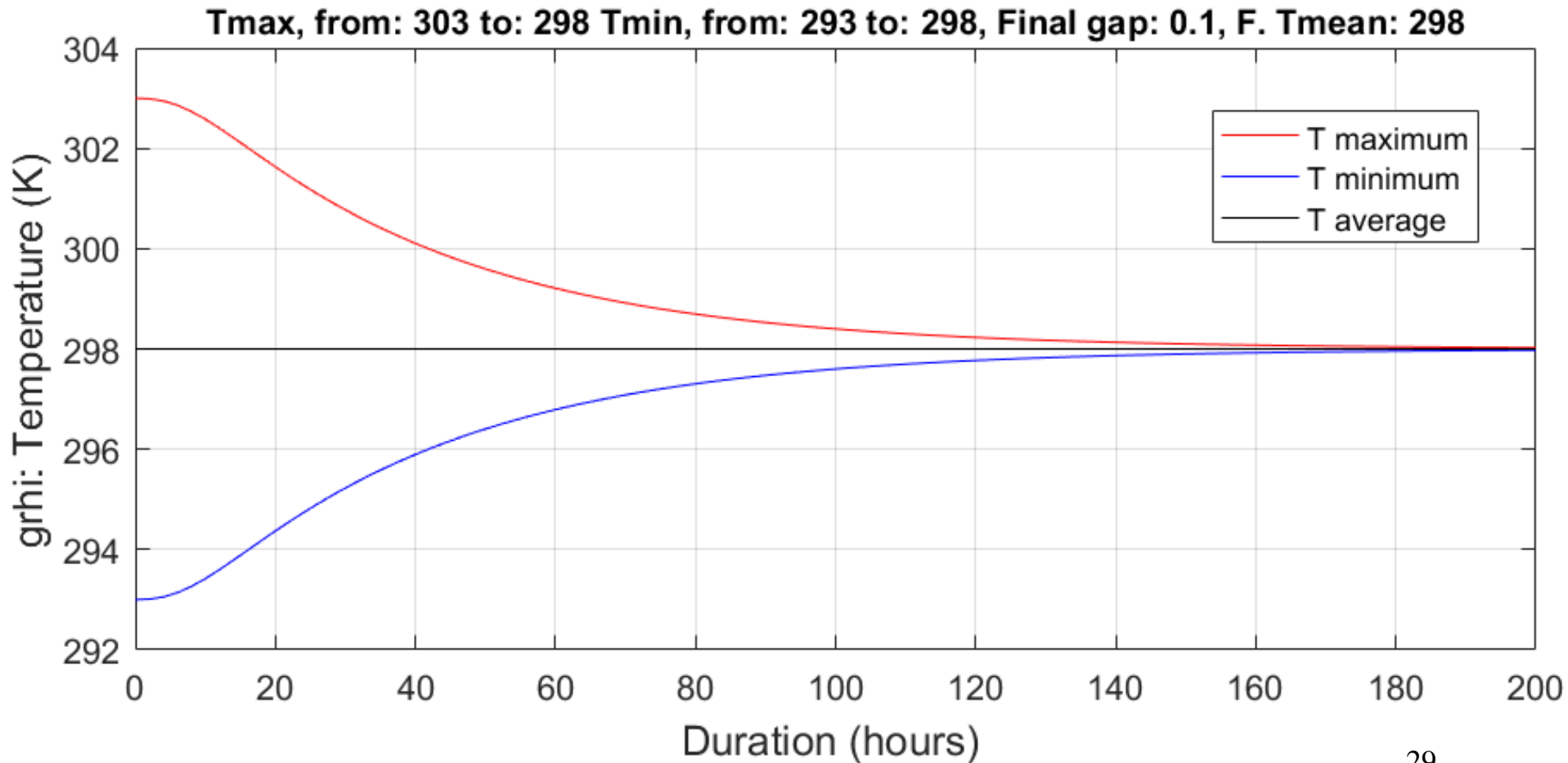
A uniform temperature test is carried out on a domain of dimensions: (1m x 0.1m x 2m) whose walls are adiabatic. Half of the area is at 303 K, the other half at 293 K.

Homogeneity of the temperature after 33. hours, the gap is decreasing by half.

Control parameter <code>pa6</code>	: 1
<code>conde.m</code> conductivity	: 2 W/(mK)
Specific heat	: 1000 J.m <sup>-3</sup> .K <sup>-1</sup>
Specific mass	: 2500 kg.m <sup>-3</sup>
Initial temperature	: 303 K
Wall base temperature	: 293 K
Domain dimensions	: 1 m x 0.1 m x 2 m
Mesh Dimension	: 21 x 42
Analyzed period	: 33. hours
Number of iterations	: 30



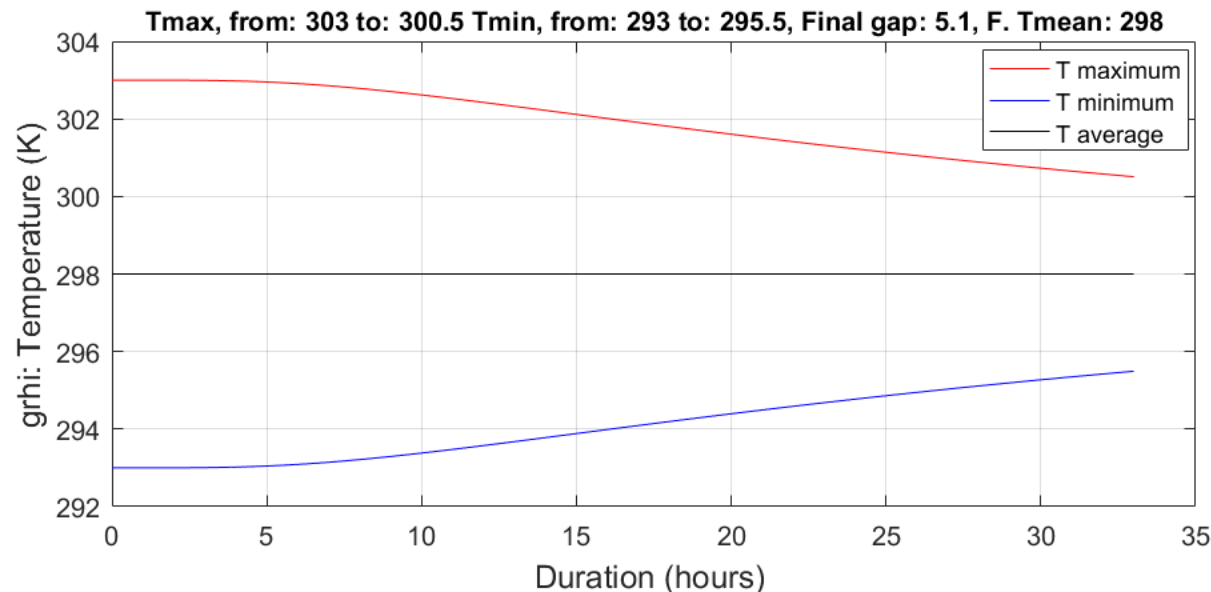
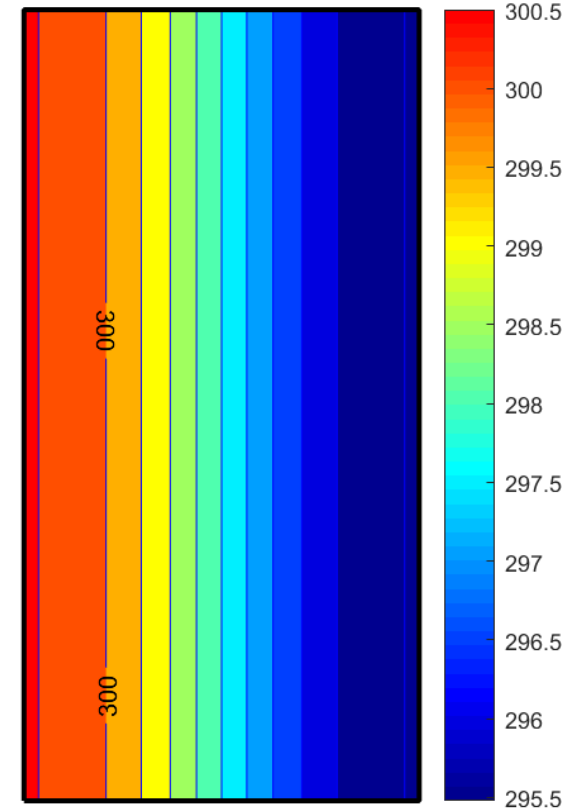
A uniform temperature test is carried out on a domain of dimensions:  $(1\text{ m} \times 0.1\text{ m} \times 2\text{ m})$  whose walls are adiabatic. Half of the area is at  $303\text{ K}$ , the other half at  $293\text{ K}$ . The time evolution and the moment at which the temperature becomes uniform are examined. The homogenization process depends on the diffusivity.



$T_{max} : 301 \text{ K}$ ,  $T_{min} : 295 \text{ K}$ ,  $pa6 : 0.5 \text{ K}$

Homogeneity of the temperature after 33. hours,  
the gap is decreasing by half.

Control parameter  $pa6$  : 1  
 $conde.m$  conductivity : 2 W/(mK)  
 Specific heat : 1000 J.m<sup>-3</sup>.K<sup>-1</sup>  
 Specific mass : 2500 kg.m<sup>-3</sup>  
 Initial temperature : 303 K  
 Wall base temperature : 293 K  
 Domain dimensions : 1 m x 0.1 m x 2 m  
 Mesh Dimension : 21 x 42  
 Analyzed period : 33. hours  
 Number of iterations : 30



The parameter

$pa6$  allows controlling the procedure:

$pa6 = 0$ . Standard situation.  $nf = nx + 1$

$pa6 = 1$ . No load, no fixation.  $t3 = 0, nf = 0$

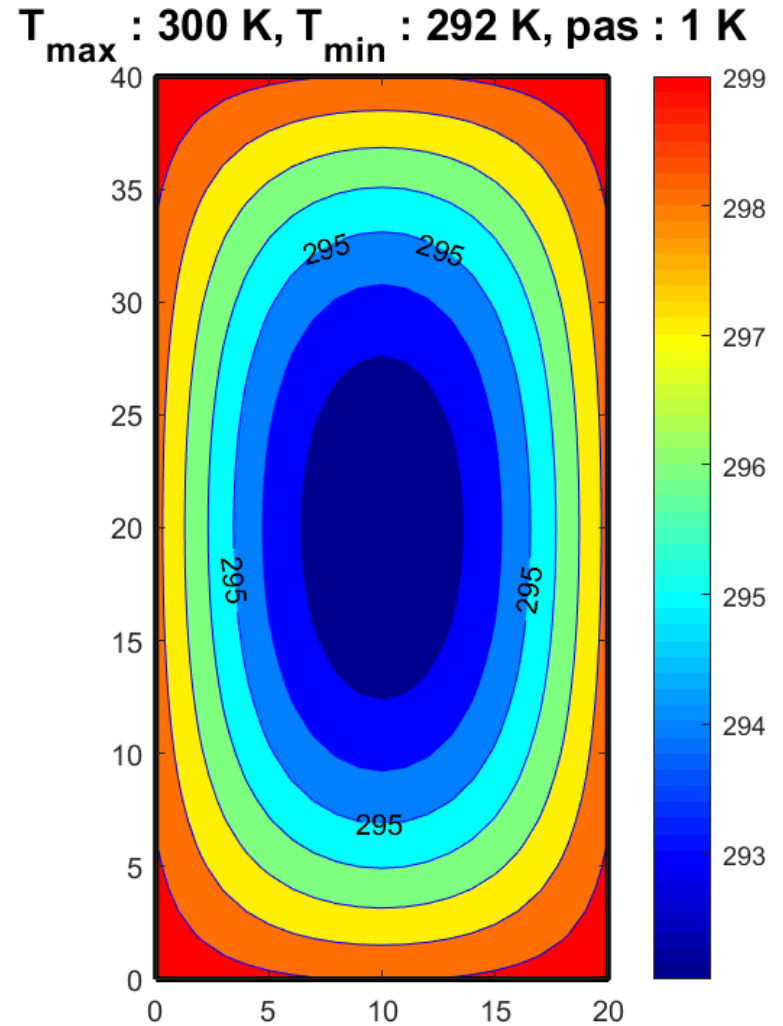
$pa6 = 2$ . Four convective nodes.  $t3 = 4, nf = 0$

## Examples:

1. Homogenization of the temperature in an adiabatic domain
2. Heating of a cold domain
3. Cooling of a hot domain
4. Convection on three sides of the domain

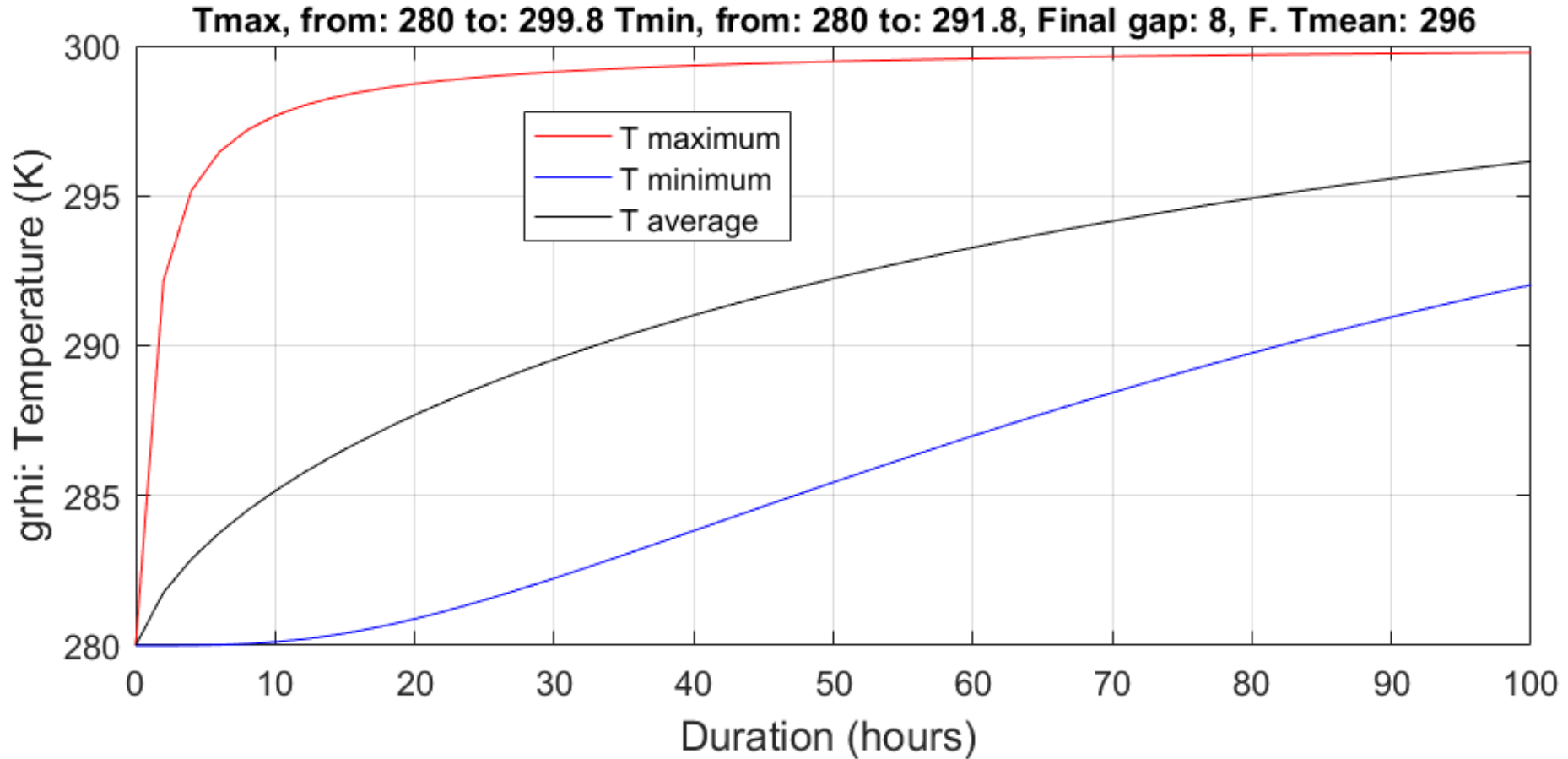
We follow with a solid immersed in a fluid at 300  $K$  with convective heat exchanges on the four sides of the solid. At the begin, the temperature of the solid is 280  $K$ . After 100  $h$ , its mean value is 296  $K$ .

```
Control param. pa6 : 2
Convection coeff. h : 25 W/(m2K)
Specific heat      : 1000 J.m-3.K-1
Specific mass     : 2500 kg.m-3
Air temperatures  : 300 300 300 K
Initial temperature : 280 K
conde.m conductivity: 1 W/(mK)
Domain dimensions : 1 x 0.1 x 2 m
Mesh size        : 20 x 40
N. virtual nodes t3 : 4
Number of fixations : 0
Domain heat capacity: 500000 J/K
Diffusivity      : 4e-07 m2/s
Total duration   : 100 h
Number of iterations: 50
N. of convective el.: 120
Virtual conv. nodes : 862 863 864 865
Stat. Ntca no nf t3 : 865 861 0 4
Cpu              : 5.13 sec.
```





The quantity of exchanged heat is equal to the product of the temperature increase by the specific heat and by the mass of the solid



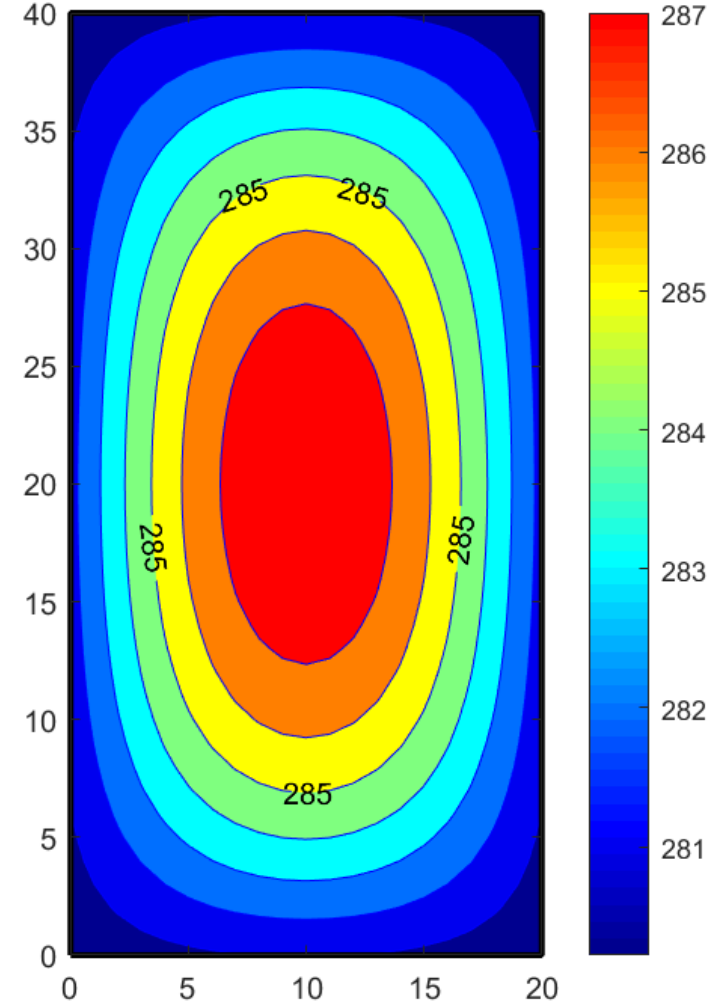
## Examples:

1. Homogenization of the temperature in an adiabatic domain
2. Heating of a cold domain
3. Cooling of a hot domain
4. Convection on three sides of the domain

We follow with a solid immersed in a fluid at 280  $K$  with convective heat exchanges on the four sides of the solid. At the begin, the temperature of the solid is 300  $K$ . After 100  $h$ , its mean value is 254  $K$ .

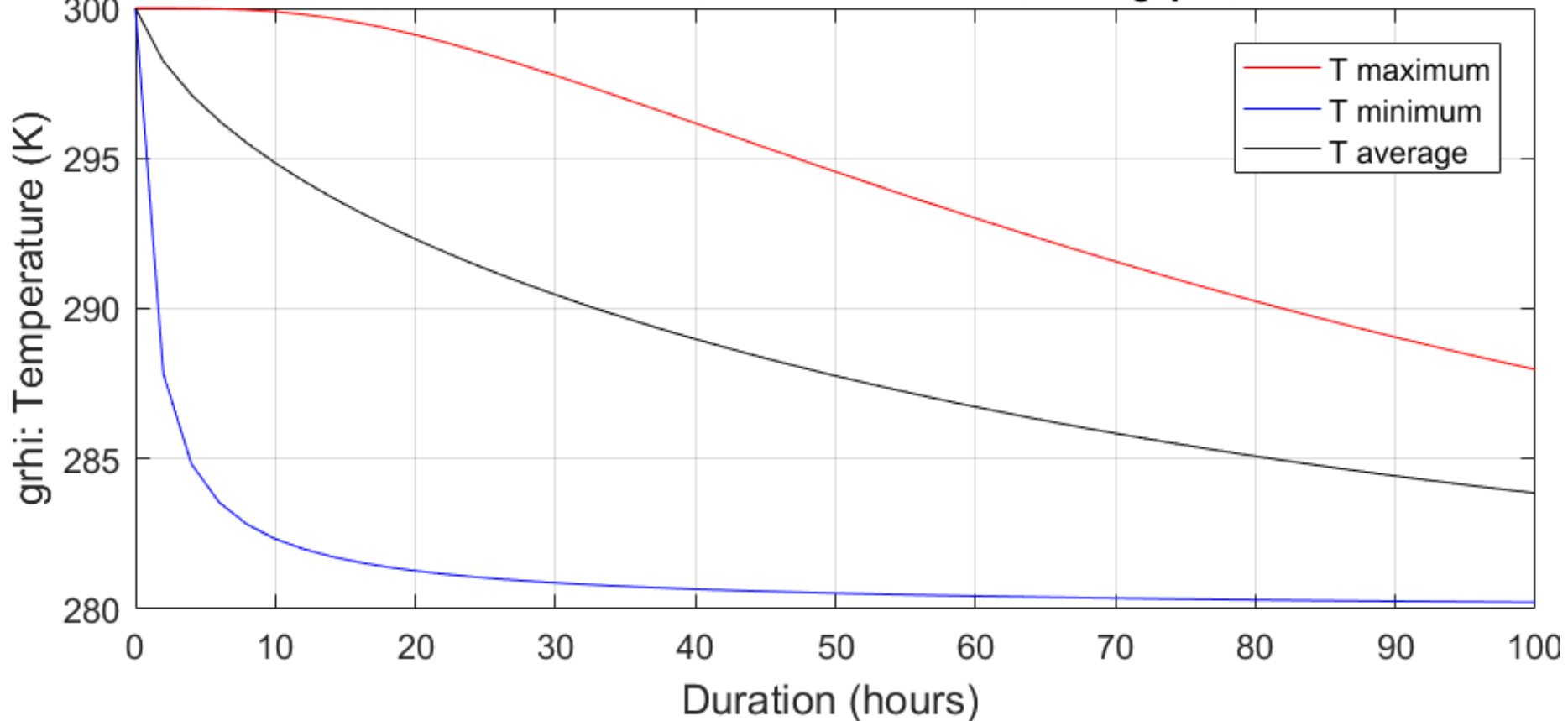
$T_{\max}$  : 288 K,  $T_{\min}$  : 280 K, pas : 1 K

```
Control param. pa6 : 2
Convection coeff. h : 25 W/(m2K)
Specific heat      : 1000 J.m-3.K-1
Specific mass     : 2500 kg.m-3
Air temperatures  : 280 280 280 K
Base temperature  : 280 K
Initial temperature : 300 K
conde.m conductivity: 1 W/(mK)
Domain dimensions : 1 x 0.1 x 2 m
Mesh size        : 20 x 40
N. virtual nodes t3 : 4
Number of fixations : 0
Domain heat capacity: 500000 J/K
Diffusivity      : 4e-07 m2/s
Total duration   : 100 h
Number of iterations: 50
N. of convective el.: 120
Virtual conv. nodes : 862 863 864 865
Stat. Ntca no nf t3 : 865 861 0 4
Cpu              : 5.05 sec.
```



The quantity of exchanged heat is equal to the product of temperature increase by the specific heat and by the mass of the solid.

**Tmax, from: 300 to: 288.2 Tmin, from: 300 to: 280.2, Final gap: 8, F. Tmean: 284**



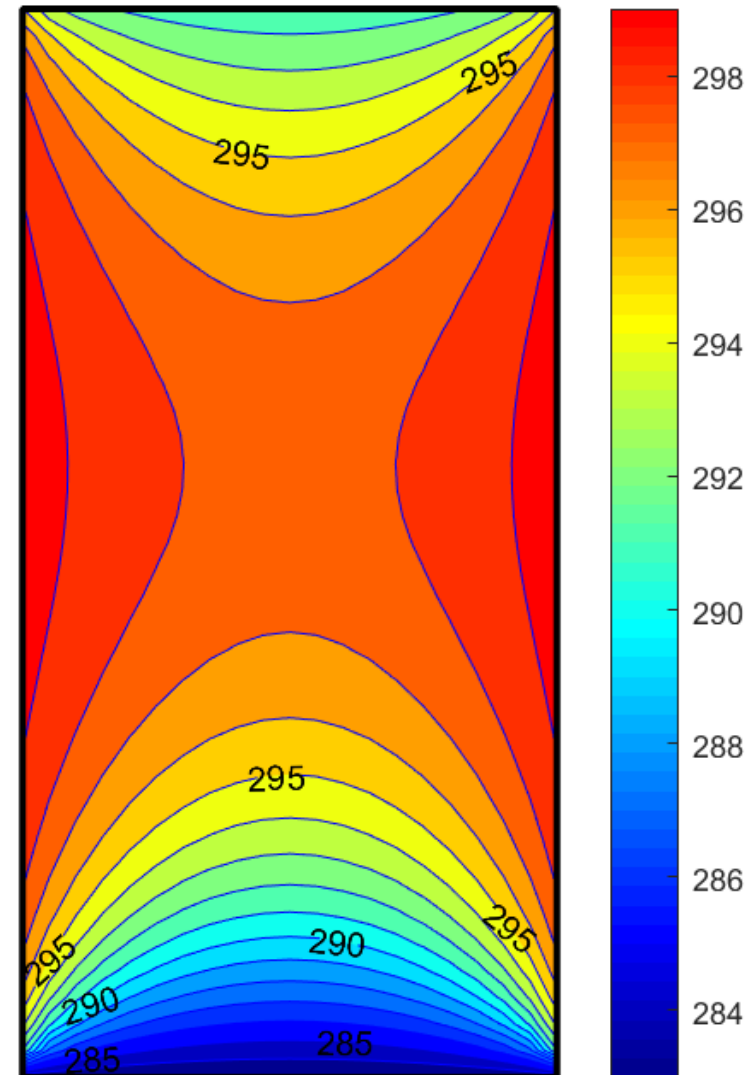
## Examples:

1. Homogenization of the temperature in an adiabatic domain
2. Heating of a cold domain
3. Cooling of a hot domain
4. Convection on three sides of the domain

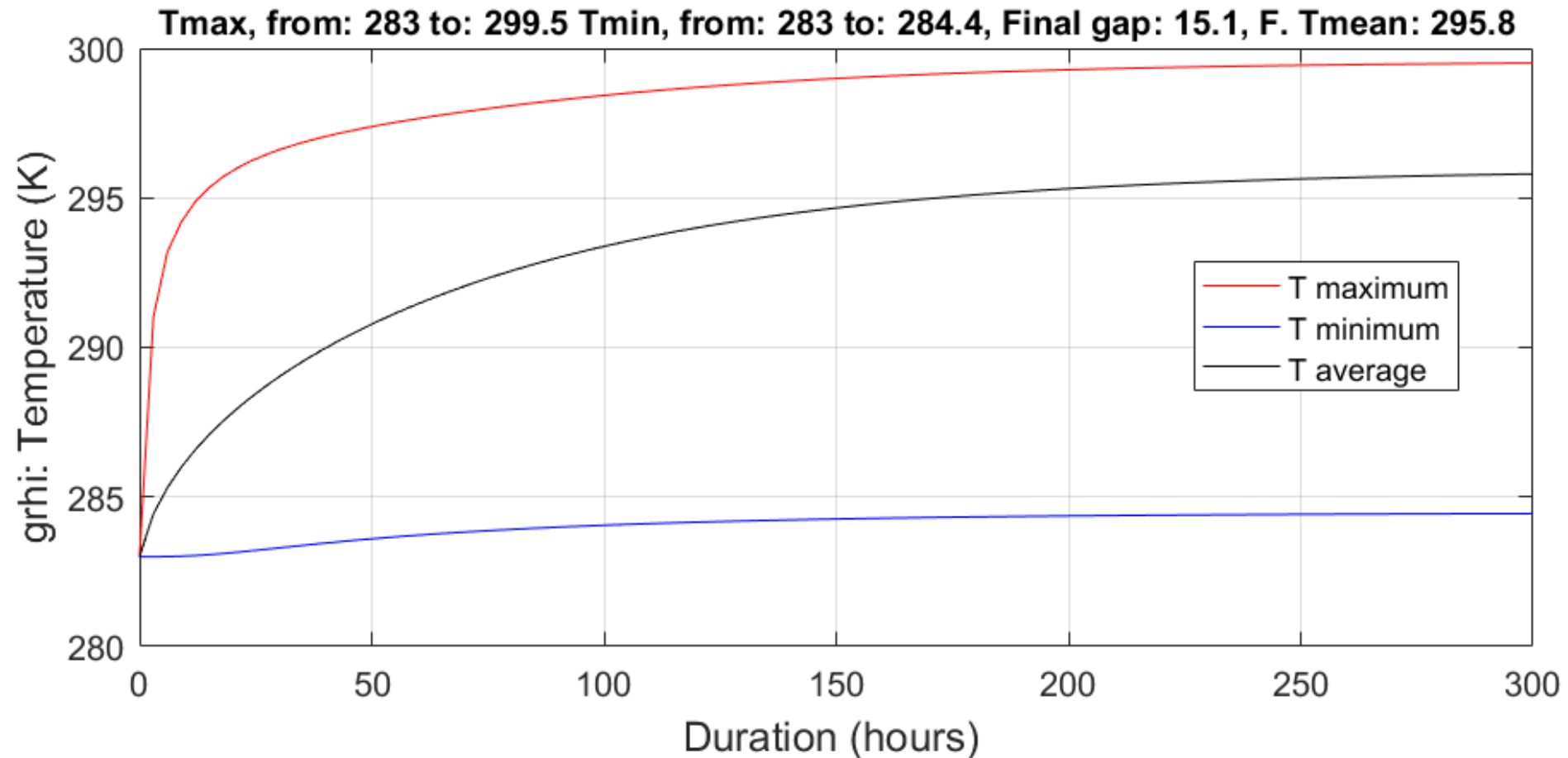
$T_{\max} : 300 \text{ K}, T_{\min} : 283 \text{ K}, \text{pas} : 1 \text{ K}$

In this example the temperature of the bottom edge of the domain is fixed at the same value as the initial temperatures while the three other sides are subjected to convection. The air temperature corresponding to the top side is 10  $K$  lower than the temperatures related to the vertical sides.

```
Control param. pa6 : 0
Convection coeff. h : 25 W/(m2K)
Specific heat      : 1000 J.m-3.K-1
Specific mass     : 2500 kg.m-3
Air temperatures  : 300 300 290 K
Base temperature  : 283 K
Initial temperature : 283 K
conde.m conductivity: 1 W/(mK)
Domain dimensions  : 1 x 0.1 x 2 m
Mesh size         : 20 x 40
N. virtual nodes t3 : 3
Number of fixations : 21
Domain heat capacity: 500000 J/K
Diffusivity       : 4e-07 m2/s
Total duration    : 300 h
Number of iterations: 100
Cpu               : 13.2 sec.
```

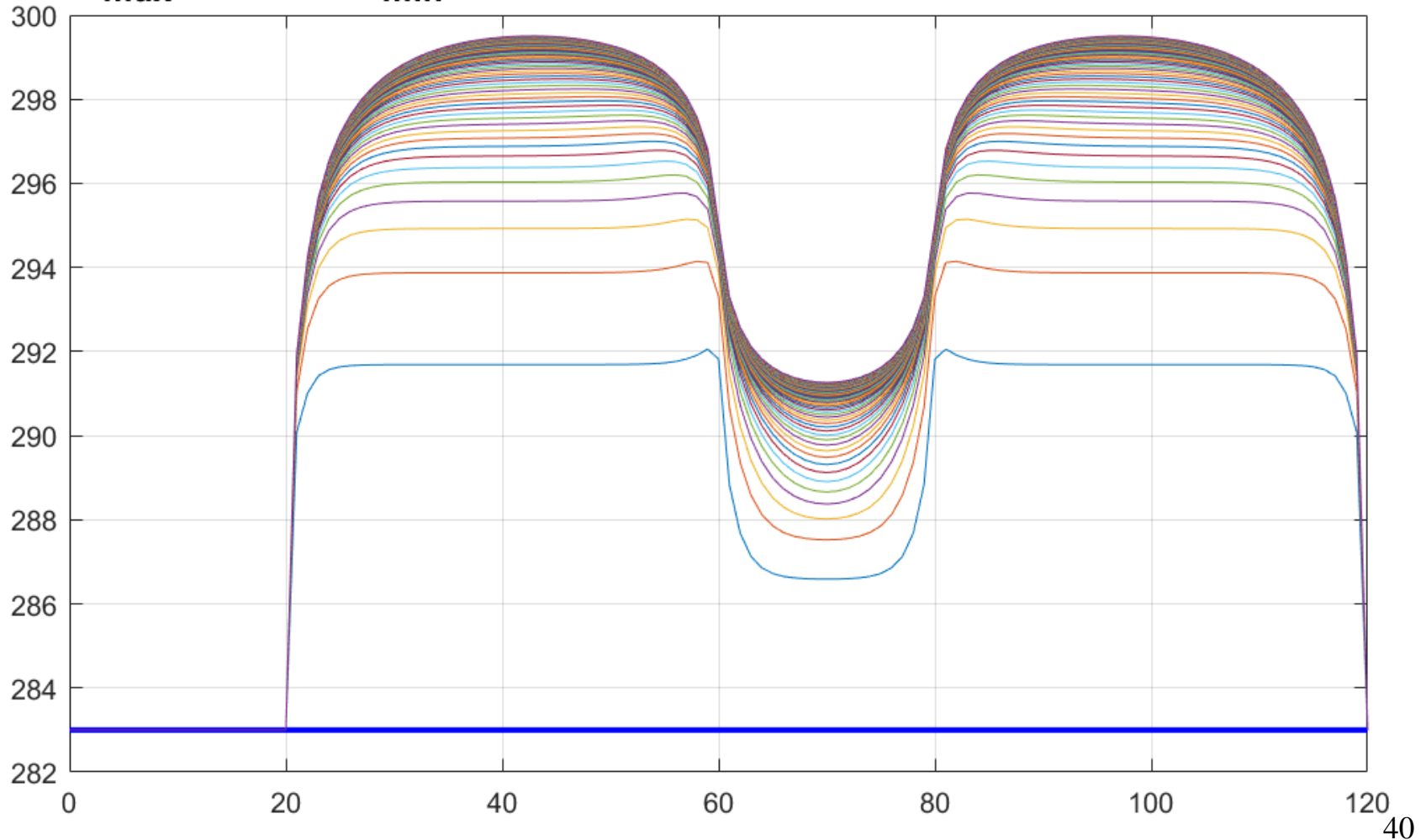


We observe the evolution of the maximum temperature of the domain from the initial one to a stabilized value of about 300 *K*. The three temperatures are computed for the internal nodes (not on the base).



In the following graphics, the temperature is shown along the perimeter of the domain, starting at the left bottom corner and moving forward with the area at the left side of the path. This curve is outlined at each time step.

**$T_{\max} = 300 \text{ K}$ ,  $T_{\min} = 283 \text{ K}$ , duration: 300 h, numb. iterations : 60**





## Procedure Matlab<sup>®</sup> pp\_transient.m for transient heat transfer

```

1  nx = 21; ni =30 ; pe =33 ; dt=pe*3600;gap=.5;           % Input data
2  pte = [290;290;303; % Sky temperature                 East, West, Top
3      303;           % Initial temperature in transient analysis
4      293;           % Wall base temperature
5      300;300;300]; % temperatures of atmosphere :      East, West, Top
6  pa6= 1           ; disp(['Control param. pa6 : ',num2str(pa6)])
7  hh = 25          ; disp(['Convection coeff. h : ',num2str(hh), ' W/(m2K)'])
8  Cp = 1000        ; disp(['Specific heat      : ',num2str(Cp), ' J.m-3.K-1']);
9  ro = 2500        ; disp(['Specific mass     : ',num2str(ro), ' kg.m-3'])
10 tb = pte(5)      ; disp(['Base temperature  : ',num2str(tb), ' K'])
11 ti = pte(4)      ; disp(['Initial temperature: ',num2str(ti), ' K'])
12 wi = 1;he=2;ep=0.1; % Width, height & thickness of the wall
13 ny = nx*2;my = ny+1;nel = nx*ny;no = (nx+1)*(ny+1); % Mesh definition
14 co = conde(nx,ny);
15 disp(['Domain dimensions : ',num2str(wi), ' x ',num2str(ep), ' x ',...
16      num2str(he), ' m'])
17 scr= 0;scs=1;sc1=2;t3=3; % N. of add. nodes for convection & radiation
18 if pa6 == 2;t3=4;tad(1:4)=[pte(6:8) pte(6)];
19   disp(['Air temperatures : ',num2str(tad), ' K'])
20 else
21   tf = pte(6:8)';disp(['Air temperatures : ',num2str(tf), ' K'])
22 end % pa6 = 2: 4 virtual convection temp.
23 if pa6 == 1;t3=0; end
24 ii = 0;
25 if scr >0;tad(ii+1:ii+3)=ts;ii=ii+3;end % Sky temperatures
26 if scs >0;ii=ii+1;tad(ii)=pte(6); end % Fluid temperature of the top
27 if sc1 >0;tad(ii+1:ii+2)=pte(7:8);end % Fluid temp. of vertical borders
28 disp(['Mesh size : ',num2str(nx), ' x ',num2str(ny)])
29 disp(['N. virtual nodes t3 : ',num2str(t3)])
30 if pa6 == 0;nf=nx+1;else;nf = 0;end % Computing the number of fixations
31 disp(['Number of fixations : ',num2str(nf)])
32 Ntca = no + t3; % Total number of nodes
33 tst = tic; % Beginning the analysis, initialisation of the timer
34 disp(['Diffusivity : ',num2str(co(1)/(ro*Cp)), ' m2/s'])
35 disp(['Total duration : ',num2str(dt/3600), ' h'])
36 disp(['Number of iterations: ',num2str(ni)])
37 C = zeros(Ntca,Ntca); % Initialization of the global capacity matrix
38 [K ] = CoKr34 (nx,ny,ep,he,hh,pa6); % Global K with convection
39 lK = loca (nx,ny);% Elem. local. matrix with fixation without convection
40 Vel = ep*wi/nx*he/ny;
41 Cel = Cp*ro*Vel/36*[4 2 1 2;2 4 2 1;1 2 4 2;2 1 2 4]; % El. capacity
42 Kel = ep/6*[4 -1 -2 -1;-1 4 -1 -2;-2 -1 4 -1;-1 -2 -1 4]; % elem. K
43 for n=1:nel
44   for i=1:4
45     for j=1:4 % Assembling nel conductivity & capacity matrices
46       K(lK(n,i),lK(n,j)) = K(lK(n,i),lK(n,j)) + co(n)*Kel(i,j);
47       C(lK(n,i),lK(n,j)) = C(lK(n,i),lK(n,j)) + Cel(i,j) ;
48     end;

```

Procedure corresponding to the second example

1. Homogenization of the temperature in an adiabatic domain
2. Heating of a cold domain
3. Cooling of a hot domain
4. Convection on three sides of the domain

The parameter

*pa6* allows controlling the procedure:

*pa6* = 0. Standard situation.

*nf* =  $nx + 1$

*pa6* = 1. No load, no fixation.

*t3* = 0, *nf* = 0

*pa6* = 2. Four convective nodes. *t3* = 4, *nf* = 0

```

24 ii = 0;
25 if scr >0;tad(ii+1:ii+3)=ts;ii=ii+3;end % Sky temperatures
26 if scs >0;ii=ii+1;tad(ii)=pte(6); end % Fluid temperature of the top
27 if scl >0;tad(ii+1:ii+2)=pte(7:8);end % Fluid temp. of vertical borders
28 disp(['Mesh size : ',num2str(nx),' x ',num2str(ny)])
29 disp(['N. virtual nodes t3 : ',num2str(t3)])
30 if pa6 == 0;nf=nx+1;else;nf = 0;end % Computing the number of fixations
31 disp(['Number of fixations : ',num2str(nf)])
32 Ntca = no + t3; % Total number of nodes
33 tst = tic; % Beginning the analysis, initialisation of the timer
34 disp(['Diffusivity : ',num2str(co(1)/(ro*Cp)), ' m2/s'])
35 disp(['Total duration : ',num2str(dt/3600), ' h'])
36 disp(['Number of iterations: ',num2str(ni)])
37 C = zeros(Ntca,Ntca); % Initialization of the global capacity matrix
38 [K ] = CoKr34 (nx,ny,ep,he,hh,pa6); % Global K with convection
39 lK = loca (nx,ny);% Elem. local. matrix with fixation without convection
40 Vel = ep*wi/nx*he/ny;
41 Cel = Cp*ro*Vel/36*[4 2 1 2;2 4 2 1;1 2 4 2;2 1 2 4]; % El. capacity
42 Kel = ep/6*[4 -1 -2 -1;-1 4 -1 -2;-2 -1 4 -1;-1 -2 -1 4]; % elem. K
43 for n=1:nel
44     for i=1:4
45         for j=1:4 % Assembling nel conductivity & capacity matrices
46             K(lK(n,i),lK(n,j)) = K(lK(n,i),lK(n,j)) + co(n)*Kel(i,j);
47             C(lK(n,i),lK(n,j)) = C(lK(n,i),lK(n,j)) + Cel(i,j) ;
48         end;
49     end;
50 end
51 disp(['Tot. cap.sum(sum(C)): ',num2str(sum(sum(C))), ' J/K'])
52 if pa6 == 1
53     tcan = ones(Ntca,1)*tb; % T. field initialization 2 subdomains
54     for i = 1:ny+1
55         for j = 1:(nx-1)/2+1; ii = (i-1)*(nx+1)+j; tcan(ii) = ti; end
56     end
57 else
58     tcan = ones(Ntca,1)*ti; % T. field initialization - genera
59 end
60 if pa6 == 0 % Standard situation : fixed base
61     tcan(no-nx:no) = tb;
62     if t3>0; tcan(Ntca-t3+1:Ntca,1)=tad(1:t3);end
63 else
64     if t3 > 0; tcan(Ntca-t3+1:Ntca,1)=tad(1:t3);end
65 end
66 tca = tcan; % if size(tca,1) < 30;disp(tca');end
67 fnpl = zeros(Ntca,1);
68 tsmax = zeros(ni,1);tmoy = zeros(ni,1);tsmin = zeros(ni,1);
69 disp(['Stat. Ntca no nf t3 : ',num2str([Ntca no nf t3])])
70 for it = 1:ni % Solution of the iterative system *****
71     if pa6 == 2
72         Kif = K(1:no-nf,no-nf+1:Ntca);
73         tca(1:no-nf)=(C(1:no-nf,1:no-nf)+dt/ni*K(1:no-nf,1:no-nf))...
74             \ (dt/ni*(-Kif*tcan(no-nf+1:Ntca))+C(1:no-nf,1:no-nf))*...

```